

# Infrared quantum-well devices

M. Zaluźny

Institute of Physics, M. Curie-Skłodowska University,  
pl. M. Curie-Skłodowskiej 1, 20-031 Lublin, Poland

## 1. Introduction

Optical devices that work at the mid- and far-infrared have variety of potential use including night vision, pollution monitoring, industrial process control, collision avoided radars in automobiles or point-to-point communications. With such a range of applications there is greater interest in developing devices that are sensitive at these wavelengths. Most mid-infrared devices are based on interband transitions (schematically indicated in Fig. 1). Thus the wavelength dependence of the detector or emitter response is determined by the energy gap ( $E_g$ ). For example, the device working at a wavelength of  $10\ \mu\text{m}$  requires a small gap  $E_g \approx \leq 0.1\ \text{eV}$ . Unfortunately, these small-band-gap semiconductors, such as HgCdTe or PbSnTe

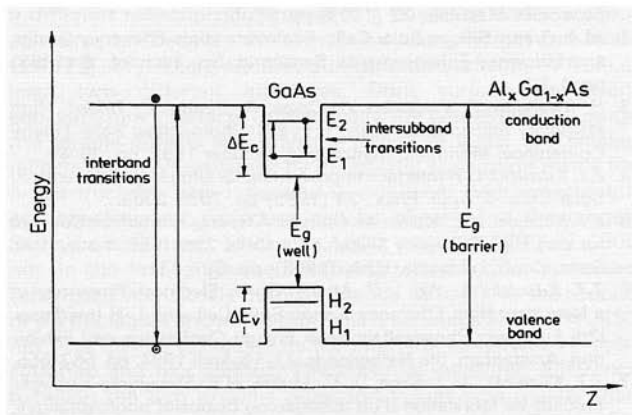


Fig. 1. Schematic band diagram of a GaAs/AlGaAs quantum well (depths  $\Delta E_c$  and  $\Delta E_v$ ). Intersubband transitions between electrons levels  $E_1$  and  $E_2$  are indicated. Conventional inter-band transitions take place between the conduction and valence bands

alloys, are notoriously hard to process and prone to the formation of effects. The above difficulties stimulated the study of novel "artificial" low "effective" band-gap materials which employ the intersubband transitions in quantum wells (QWs) based on larger-band-gap ( $E_g \geq 1\ \text{eV}$ ) semiconductors [1-4]. The QW consists of ultrathin sandwiches, made out of nanometer-thick semiconductors (mainly  $A_3B_5$  alloys) with different energy gap (see Fig. 1). This radically new scheme makes free the infrared (IR) devices from the energy gap dependence and enables to cover a broad-wavelength range from the mid-IR to the far-IR the same combination of wider-band-gap, technologically matured materials, by simple changing the QW thickness.

In an article as this one it is impossible to cover all the important areas connected with the infrared quantum well devices. Instead, we restrict to the brief review of the progress in the use of the intersubband transitions in infrared detectors and emitters. Information on the other interesting intersubband phenomena such as nonlinear optics can be found, for example, in [5] and [6].

## 2. Quantum-well infrared photodetector

The possibility of using GaAs/AlGaAs multiple quantum-well structures to detect IR was first suggested in 1977 by Esaki and Sasaki. Their idea was based on the fact that the quantum well can be treated as a well known particle-in-a-box problem. Thus the positions of the energy levels, the "subbands", are determined by the height ( $\Delta E_c$ ) and width ( $L_w$ ) of the well. For infinitely high barriers and parabolic bands the intersubband transition energy between the lowest ( $E_1$ ) and first excited state ( $E_2$ ) in conduction band is given by  $E_{21} = 3\hbar^2\pi^2/2m^*L_w^2$  where  $m^*$  is the electron effective mass in the quantum well. Consequently, by tailoring the quantum well

structure, it should be possible to achieve the situation when photon energy  $h\omega$  coincides with  $E_{21}$  (Strong intersubband absorption was observed for the first time by West and Eglash in 1985 [2]. Electrons were introduced by doping the barrier materials.) The important feature of the intersubband transitions is that the optical electric field must have a component parallel to  $z$  in order to induce an intersubband absorption. Consequently, the normal incident radiation will not be absorbed.

After absorption of the infrared photon, the photoelectron can either be transported along the quantum-well direction (with an applied parallel bias voltage), or perpendicular to the wells (with an applied electric field along the  $z$ -direction). Perpendicular transport is superior to parallel transport since the difference between the excited-state and ground-state mobilities is much larger in the latter case, thus the photoresponse should be substantially greater. For this reason the perpendicular transport of photoexcited electron was employed in the first the quantum-well infrared photodetector (QWIP) build by Levine [2]. In such geometry the photoexcited electrons tunnel out of the well and are transported in the continuum above the barriers producing a photocurrent. Unfortunately, besides the photocurrent, the detector also produces a dark current (see Fig. 2) which limits the QWIP performance. There are three contributions to this current: (i) quantum mechanical sequential tunneling from well to well through the  $\text{Al}_x\text{Ga}_{1-x}\text{As}$  barriers which dominates at the low temperature ( $\leq 30$  K); (ii) thermally assisted emission, which involves thermal excitation within the well followed by tunneling into the continuum, dominates between and 30 K and 45 K (iii) classical thermionic emission into the continuum is the main contribution to the dark current above 45 K.

In the above type QWIP the intersubband absorption excites the electron to the second bound state. The absorption to the continuum above the top of the barriers is very weak, since most of the oscillator strength is concentrated in the bound-to-bound transitions [2]. However, by decreasing the width of the quantum well, the strong oscillator strength of the excited bound state can be pushed up into the continuum resulting in a strong bound-to-continuum absorption. The major advantage of this is that the photoelectrons do not have to tunnel through the barrier to reach the continuum. In addition, the barrier thickness can now be substantially increased leading to significant reduction of the ground-state sequential tunneling (the dark current). This device exhibited an order of magnitude improvement in performance compared with bound-to-bound devices. The further improvement of the performance was possible by building a device which has the first excited state at the top of the well. Bound-to-quasi-continuum transitions maximize the intersubband absorption and maintain simultaneously the excellent electron transport properties.

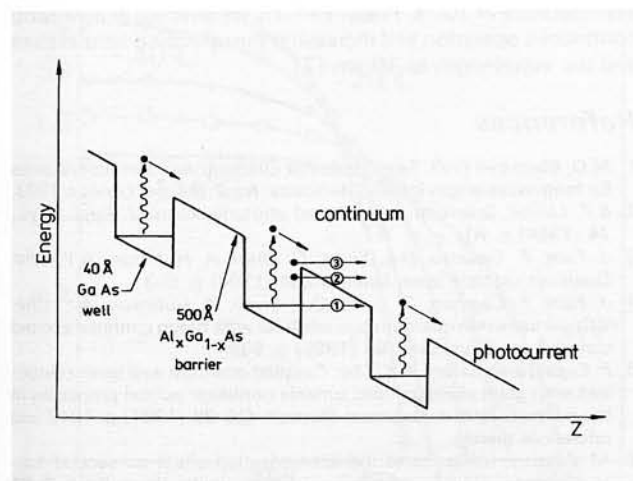


Fig. 2. Conduction band diagram in a bound-to-continuum QWIP, showing the photoexcitation and hot-electron transport process. Three "dark current" mechanisms are also shown: ground-state sequential tunneling (1); thermally assisted tunneling (2); and thermionic emission (3)

For example, bound-to-quasi-continuum transitions QWIP with peak wavelength  $\lambda_p = 15 \mu\text{m}$  typically consist of 50 quantum wells with  $L_w \approx 65 \text{ \AA}$  and  $600 \text{ \AA}$  thick ( $\text{Al}_{0.15}\text{Ga}_{0.85}\text{As}$ ) barriers. The doping density in the wells is about  $2 \times 10^{17} \text{ cm}^{-3}$ .

As it was mentioned, the quantum-mechanical selection rules for the intersubband transitions require a component of the optical electric field along the direction. One way to overcome this problem is to place gratings on the top of the detector which deflect the incoming light away from the direction normal to the surface. The grating can be made by: (i) depositing fine metal strips on top of the structure or (ii) etching grooves in a cap layer. A light-coupling efficiency can be further improved replacing the linear gratings by two dimensional grating and introducing an optical cavity which can be produced by placing a thin GaAs "mirror" below the quantum well structure. The gratings with waveguide cavity can be combined with arrays of microlenses to obtain substantial improvement in QWIP characteristics. The microlenses can focus all radiation incident on the pixel area onto a small active QWIP area. This gives the same responsibility but reduces dark current.

The performance of the photodetectors is usually described by detectivity (= the signal-to-noise ratio normalized to unit area and unit bandwidth). In the case of QWIP the noise is produced by the dark current. Thus, unlike narrow-band-gap detectors (in which noise rather weakly depends on temperature at low temperature), the performance of the QWIP improves as it is cooled. In the temperature range of  $40 \div 77$  K their detectivity is comparable with HgCdTe detectors [2]. The important strengths of QWIP are highly advanced material system which allows to produce two-dimensional imaging arrays (with of pixels or more) with non-uniformity ( $< 0.1\%$ ) which can not be achieved for the narrow-band-gap detectors. At the end we note that QWIP can be easily integrated with read-out electronics. Thus in the near future we can expect high-sensitivity, large-area and low-cost QWIP imaging arrays.

### 3. Quantum wells in semiconductor diode lasers

Now we discuss the application of QWs in semiconductor diode lasers working in the infrared. When appropriate electric field is applied across a multi-quantum well structure, the ground level  $E_1(n)$  of the  $n$ -th quantum well can be brought almost or exactly on resonance with the second level  $E_2(n+1)$  of the  $(n+1)$ -th quantum well. In such a case, electrons in the  $E_1(n)$  level can flow into  $E_2(n+1)$  and then relax to the  $E_1(n+1)$  level (Fig. 3). Some time ago, Kazarinov and Suris considered such a cascade transport for the first time [2] and pointed out that it may lead to the emission of infrared radiation. They have

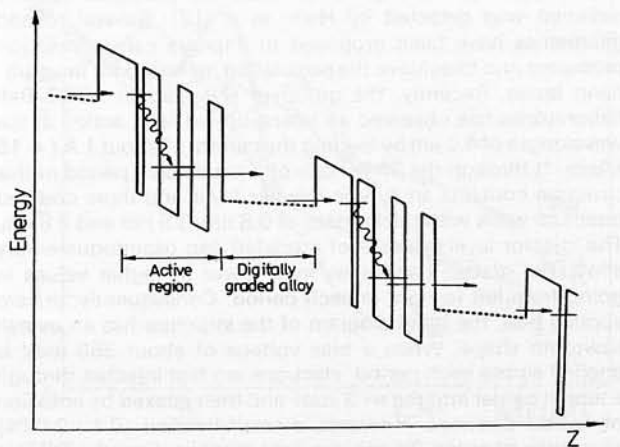


Fig. 3. Conduction band energy diagram of a portion of the 25-period (active region plus injector) section of the quantum cascade laser grown by MBE with the  $\text{Al}_{0.48}\text{In}_{0.52}\text{As}/\text{Ga}_{0.47}\text{In}_{0.53}\text{As}$  heterojunction materials. The wavy arrows indicate the laser transitions [3]

shown that the emission should occur if  $E_1(n)$  is biased slightly above  $E_2(n+1)$ . Although quite weak, the predicted infrared radiation was detected by Helm et al. [2]. Several refined geometries have been proposed to improve carrier injection processes and to achieve the population inversion for intersubband lasers. Recently, the group of scientists at AT&T Bell Laboratories has observed an intersubband laser action at the wavelength of  $4.2 \mu\text{m}$  by feeding the current of about 1 A ( $\approx 15 \text{ kAcm}^{-2}$ ) through the 25 periods of a novel structure. Each period of this structure contains an  $n$ -type injector layer and three coupled quantum wells with thicknesses of 0.8 nm, 3.5 nm and 2.8 nm. The injector layer consists of a graded gap pseudoquaternary alloy. The graded gap varies from lower to higher values in going from left to right in each period. Consequently, at zero applied bias, the band diagram of the structure has an overall sawtooth shape. When a bias voltage of about 350 meV is applied across each period, electrons are first injected through a tunnel barrier into the  $n=3$  state and then relaxed by emission of optical phonons. However, a small fraction ( $0.1 \div 0.03\%$ ) also emits photons. To achieve light amplification, the QW are designed so that the  $n=3$  state is more populated than the lower one ( $n=2$ ); the role of the  $n=1$  state is to siphon electrons fast enough out of the  $n=2$  level into the "injector" region. The present quantum-cascade laser ( $4.3 \mu\text{m}$ ) has so far operated

only in pulsed mode with a peak power of 30 mW at a temperature of 100 K. Present efforts are directed at achieving continuous operation and increasing the operating temperature and the wavelength to  $10 \mu\text{m}$  [7].

## References

1. *M.O. Manasreh (ed): Semiconductor quantum well and superlattices for long-wavelength infrared detectors.* Atech House, London 1993.
2. *B.F. Levine: Quantum-well infrared photodetectors.* J. Appl. Phys., **74** (1994) p. R1.
3. *J. Faist, F. Capasso, D.L. Sivco, C. Sirtori, A. Hutinson, A.Y. Cho: Quantum cascade laser.* Science **264** (1994) p. 553.
4. *J. Faist, F. Capasso, C. Sirtori, D.L. Sivco, A. Hutinson, A.Y. Cho: Vertical transition quantum cascade laser with Bragg confined excited states.* Appl. Phys. Lett., **66** (1995) p. 538.
5. *F. Capasso, C. Sirtori, A. Y. Cho: Coupled quantum well semiconductors with giant electrical field tunable nonlinear optical properties in the infrared.* IEEE J. Quantum Electron. **QE-30** (1994) p. 1313 and references therein.
6. *M. Zalužny: Influence of the depolarization effect on second-harmonic generation in asymmetric quantum wells.* Phys. Rev., **B 51** (1995).
7. *C. Sirtori, J. Faist, F. Capasso, D.L. Sivco, A.L. Hutchinson, A.Y. Cho: Quantum cascade laser operating at  $8.4 \mu\text{m}$  wavelength.* Appl. Phys. Lett. (in press).